Analytical Methods

A pilot study in humans of microneedle sensor arrays for continuous glucose monitoring

Journal:	*Analytical Methods*
Manuscript ID	AY-ART-02-2018-000264
Article Type:	Paper
Date Submitted by the Author:	02-Feb-2018

Complete List of Authors:	Sharma, Sanjiv; Imperial College London, Chemistry El-Laboudi, Ahmed; Imperial College London Reddy, Monika; Imperial College London Jugnee, Narvada; Imperial College London Sivasubramanyam, Sujan ; Imperial College London el-Sharkawy, Mohamed; Imperial College London Georgiou, Pantelis; Imperial College London Johnston, Desmond; Imperial College London Oliver, Nick; Imperial College London Cass, Anthony; Imperial College of Science, Centre for Biotechnology

A pilot study in humans of microneedle sensor arrays for continuous glucose monitoring

Sanjiv Sharma [a, *, ‡], Ahmed El-Laboudi [b], Monika Reddy [b], Narvada Jugnee [b], Sujan Sivasubramanyam [b], Mohamed El Sharkawy [c], Pantelis Georgiou [c], Desmond Johnston [b], Nick Oliver [b], Anthony EG Cass [d *]

[a] *Department of Chemistry & Institute of Biomedical Engineering, Imperial College London SW7 2AZ (U.K)*

[b] *Division of Diabetes, Endocrinology & Metabolism, Imperial College London, W2 1PG (U.K)*

[c] *Department of Electrical and Electronic Engineering, Imperial College London, SW7 2AY (U.K)*

[*] To whom correspondence should be addressed.

E-mail address: sanjiv.sharma@imperial.ac.uk / t.cass@imperial.ac.uk

Tel: +44 (0) 207 594 1595

[‡] *Current address: College of Engineering, Swansea University Bay Campus, SA1 8EN (U.K)*

Abstract

Although subcutaneously implanted continuous glucose monitoring (CGM) devices have been shown to support diabetes self-management, their uptake remains low due to a combination of high manufacturing cost and limited accuracy and precision arising from their invasiveness. To address these points, minimally invasive, solid microneedle array-based sensor for continuous glucose monitoring is reported here. These intradermal solid microneedle CGM sensors are designed for low cost manufacturing. The tolerability and performance of these devices is demonstrated through clinical studies, both in healthy volunteers and participants with type 1 diabetes (T1D). The geometry of these solid microneedles allows them to penetrate dermal tissue without the need for an applicator. The outer surface of these solid microneedles are modified as glucose biosensors. The microneedles sit in the interstitial fluid of the skin compartment and monitor real-time changes in glucose concentration. Optical coherence tomography measurements revealed no major axial movement of the microneedles in the tissue. No significant adverse events were observed and low pain scores were reported when compared to catheter insertion, deeming it safe for clinical studies in T1D. These amperometric sensors also yielded currents that tracked venous blood glucose concentrations, showing a clinically acceptable correlation. Studies in people with T1D gave a mean absolute relative difference (MARD) of 9% (with respect to venous blood glucose) with over 94% of the data points in the A and B zones of the Clarke error grid. These findings provide baseline data for further device development and a larger clinical efficacy and acceptability study of this microneedle intradermal glucose sensor in T1D.

Abbreviations

CGM, continuous glucose monitoring; T1D, Type 1 Diabetes; CEG, Clarke Error Grid; MARD, mean absolute relative deviation, PARD, Precision average relative deviation; ISF: Interstitial fluid, Optical coherence tomography (OCT).

Keywords

Diabetes, glucose biosensor, optical coherence tomography, skin interstitial fluid (ISF), minimally invasive

Continuous glucose monitoring (CGM) sensors provide real-time information on glucose concentration, and its rate and direction of change. Their use is associated with an improvement in glucose control in adults and children with type 1 diabetes (T1D),[1] reducing the risk of hypoglycaemic and hyperglycaemic episodes. However, the adoption of CGM remains low when compared with insulin pump therapy.[2] This is attributed to the challenges associated with long term use of subcutaneous CGM devices. The devices measure subcutaneous interstitial fluid (ISF) glucose concentrations using sensing wires inserted through a hollow needle using an applicator. Implantation in the subcutaneous tissue for 7-14 days is associated with biofouling which may adversely impact accuracy, one of the barriers to their continued use. [2] In addition, high manufacturing costs mean each sensor is relatively expensive and may not be eligible for reimbursement. Other factors that adversely affect the wider adoption of CGM sensors are pain associated with both the initial implantation and the continued use of the devices [3] as well as their poor tolerability.[4]

Microneedles have been extensively used for therapeutic drug and vaccine delivery applications.[5-7] It is only in the recent years that they have been extended for diagnostic applications. As in the drug delivery applications, the microneedles are mainly used to disrupt the *stratum corneum* layer of the skin, the first step towards sampling interstitial fluid. Various approaches have been used to extract the skin ISF and measure glucose and other metabolites. These include the use of microdialysis probe[8, 9] and hollow microneedles[4]. These reported devices have often relied on extractive sampling glucose in the skin compartment by passive diffusion[4] or using reverse iontophoresis [10] or ultrasound [11] but are limited by transport of glucose from the ISF to the sensor located on the skin surface. Hollow microneedles for glucose measurement either involve the use of the lumen as the sensing surface or the use of a reservoir to extract and measure. Such devices are not only challenging to fabricate using high throughput methods but also are prone to blocking of the lumen.[4] Eltayib et.al. have reported the used of hydrogel-based microneedles for extracting skin (ISF) in rats to measure lithium.[12] The potential applications of minimally invasive, microneedle-based sensors have been reported elsewhere.[13-16]

We have previously introduced solid microneedles that avoid potential problems associated with the extraction of skin ISF by hollow microneedles. [17-21] These microneedle arrays are mainly based on strategies to make them less painful, less conspicuous, and easier to apply, wear and replace. In order to access the ISF, microneedle geometry and the subsequent

penetration depth are optimised to yield devices which result in either little or no pain. Technologies that allow low cost fabrication of accurate CGM sensors that can be used over shorter periods (24-48 hours) will reduce the risk of encapsulation seen with subcutaneous sensors that are typically implanted for a longer period, improving both effectiveness and uptake of CGM devices.

More importantly, microneedle array glucose sensors also offer the potential to enhance sensor accuracy through simultaneous multiple glucose measurements [22] and by determining glucose concentrations in dermal ISF rather than subcutaneous ISF, since the dermal ISF glucose concentration is more similar to that of the blood and suffers from less lag when compared to subcutaneous ISF glucose.[23]

We present here for the first time, solid microneedle array based minimally invasive, continuous glucose monitoring systems optimised through *in vivo* studies in human. These solid microneedle array for minimally invasive, intradermal continuous glucose monitoring (CGM) sensor were evaluated over three phases involving 14 healthy volunteers and 10 participants with type 1 diabetes (T1D) for tolerability and the performance of our sensing devices. Here we report the results from the novel devices based on the clinical evaluations.

Experimental Section

Ethics

The protocol and informed consent documents were approved by the research ethics committee, NHS health research authority (REC reference: 16/LO/0007, IRAS project ID 190530). All participants provided written informed consent prior to participation in the study protocol.

The CGM devices comprise four individual arrays of microneedles, made from polycarbonate, three were metallised with platinum and one with silver to obtain the working and reference electrodes respectively. Electrical contacts were then made by wire bonding using silver paint and epoxy, in preparation for further functionalization to render them sensitive to glucose. The silver coated microneedles were modified to a Ag/AgCl reference electrode using a saturated solution of ferric chloride ($FeCl_3$). The platinum microneedles were functionalised with an electropolymerised polyphenol film, entrapping glucose oxidase. Details of the methods have been described previously. [17, 19, 20] The hydrogen peroxide

generated by the enzyme reaction was measured at the electrode surface from the oxidation current, initially at 0.7V. In the final phase, the sensors were biased at 0.5V to reduce the contribution from possible interfering species in the tissue.

The microneedle arrays were sterilised with 25 kGy of ^{60}Co radiation (Synergy Health) following determination of the bio-burden levels. These studies were performed in accordance with ISO 11137-2:2012, Sterilisation of Health Care Products-Radiation-Part2: Establishing the Sterilisation dose.

All CGM devices were inserted into the forearm of the volunteers by application of moderate thumb pressure for 1 minute. Once inserted, the devices were secured using 3M Tegaderm tape.

Study design and setup for clinical evaluation

The main objective of the clinical study was to evaluate intradermal continuous glucose monitoring devices firstly by ascertaining the safety and tolerability in healthy participants and then by measuring performance in participants with T1D by comparing the output current against a standard laboratory method (figure 1).

Insert Figure 1 here

Phase 1: Healthy volunteers, 6 hours (Tolerability of microneedle arrays)

The microneedle arrays described above were inserted in healthy volunteers for 6 hours to assess the tolerability of the devices. 3 volunteers were of Caucasian race, 3 of Asian race, 1 Middle Eastern and 1 of mixed race. Volunteers were 34.6 ± 6.9 years old (range 23-48 years). The devices were then removed and pain scores recorded using a Visual Analogue Scale (VAS). To measure tolerability, a 100mm-VAS was used to assess pain resulting from microneedle arrays (at insertion and throughout the study) in comparison to pain resulting from insertion of a 20-G intravenous cannula (Venflon). The pain intensity score was measured immediately after sensor and intravenous cannula application at the beginning of the study, and immediately after sensor removal, in all of the clinical studies.

Phase 2: Healthy volunteers, 24 hours (Tolerability and penetration depth of microneedle arrays)

In Phase 2, the microneedle arrays were inserted in healthy volunteers for 24 hours to assess both tolerability and skin penetration. Most of these volunteers participated in Phase1. To determine both the depth of penetration and how well they remain seated in the skin compartment, a non-invasive imaging technique, Optical Coherence Tomography (OCT), (VivoSight Dx, Michelson Diagnostics Ltd, (U.K)) was used. Based on light scattering in the different layers of skin, this technique produces cross sectional images of distinct layers of the skin and has previously been used for insertion studies of microneedles.[24]

Polycarbonate microneedle arrays with a 1 mm thick base were masked selectively to prevent metallisation and yield transparent structures which could then be used for imaging (Figure 2). A probe standoff (provided by Michelson diagnostics) was used to aid positioning the probe on the base of the microneedle inserted in the skin for setting the correct scan distance. Care was taken not to apply too much pressure on the microneedle base, to prevent undue additional pressure on the tissue. The OCT images were acquired at the start and after 6 and 24 hours of the study. It involved measuring the gaps/air pockets between the microneedle base plate and *stratum corneum*. This data was analysed using Kruskal-Wallis ANOVA.

Insert Figure 2 here

Phase 3: Participants with Type 1 Diabetes, 24 hours (Performance of microneedle arrays)

In Phase 3, 10 participants were recruited. 9 were of Caucasian race, and 1 of mixed race. Participants were 38 ± 16 years old (20 and 65 years) of age. Pain scores were recorded using a Visual Analogue Scale (VAS) for the microneedle CGM device, IV cannula and a commercially available CGM (Dexcom G4 Platinum) device. To measure the performance of the microneedle devices in T1D participants, both a commercially available and an in house built potentiostat were used. The commercially available potentiostats used here included: (1) CHI 1030b potentiostat (CHI Instruments) (Figure 3a) and (2) an EmStatBlue (PalmSens) (Figure 3b). The CHI potentiostat was run on general-purpose electrochemical software (GPESv4) for the chronoamperometric measurements. The EmStatBlue potentiostat was connected to a multiplexer (Mux) and a battery pack via cables and housed in a bag to make it more portable. A hand held android tablet (Samsung Galaxy Tab 2 7inch) was used to run the PS Trace 4.7 program. The potentiostat connected to the tablet via Bluetooth and was used to continuously bias the inserted microneedle array working electrodes at 0.7V against

the integrated microneedle array reference electrode with a data point being collected every 60 seconds.

Insert Figure 3 here

An in-house built, printed circuit board based device[25,26], comprising a single channel potentiostat, a microcontroller and a microSD card was used to apply a potential, record and process the data during Phase 3 as shown in Figure 3(c). This potentiostat continuously biased the inserted microneedle array sensors at 0.5V against the integrated reference electrode with a data point being collected every 10 seconds, the currents were then filtered and averaged over 5 minutes, as described earlier.[26]

Venous blood was sampled every 30 minutes using a catheter (Venflon) and glucose concentrations were determined by a reference laboratory method (YSI Glucose Analyzer). The performance of our devices was assessed from the chronoamperometry data. In the double axis plot, the abscissa represents time and the two ordinate axes represent current and YSI glucose concentration (Figure 6). The microneedle CGM currents were calibrated against YSI venous blood glucose readings. In studies involving the use of EmStatBlue, the calibration was done as a single point calibration wherein the highest value of the venous blood reading corresponded to the highest value of current. If these values coincided at the same time then it was assumed that there was no lag between the two. In instances, where the values did not coincide at the same time, the time difference between these readings gave us the time lag between glucose concentrations in venous blood and subdermal space.

In studies with the PCB based potentiostat, calibration was performed two hours post-insertion wherein the current value at that point was calibrated against the venous blood value at the same point of time. In Phase 3, 10 participants with Type 1 diabetes were recruited for clinical studies on the microneedle array based continuous glucose monitoring sensors. The sensors were tested for their function post *removal* with known concentration of glucose solution (5, 10 and 20 mM). This was then used as a criterion for deciding which of the sensors retained function during the studies. Based on this, data from 8 individuals was deemed suitable for analysis.

The sensor connectors, comprising of wires held by crocodile clip connector appeared to be the weak link in the setup and became disconnected during the night. Due to this technical challenge, only electrochemical data collected during the day time when there had been no

reported connection failure have been considered for analysis. The microneedle CGM devices mostly got disconnected during the night time (after nearly 12-15 hours from the start of the study). During Phase 3 venous blood was sampled every 30 minutes during the day and hourly at night, which limited the number of data points for Clarke Grid error analysis to 205. Data analysis of the microneedle sensor performance was performed retrospectively.

Statistical analysis

Analysis of optical coherence tomography data using Kruskal-Wallis ANOVA

The optical coherence data obtained through frequent measurements was analysed using the Kruskal-Wallis ANOVA analysis using the Wizard application (www.wizardmac.com) running on an iMac. This was used to calculate the median values (Figure 5).

Evaluation of clinical accuracy using Clarke Error Grid Analysis

The comparison of YSI reference blood glucose values against our CGM device values was analysed using Clarke Error Grid (CEG)[27, 28] using the MatLab routine Clarke Error Grid Analysis.[29] The double plots of the current values obtained from chronoamperometry measurements and the YSI readings. The sensors that showed poor correlation were tested post studies to assess their functionality. In cases where the sensors showed a complete loss of function in the post clinical study tests, the data was not considered for analysis. Similarly, in studies where there were technical issues with disconnection of the CGM sensing device and the potentiostat especially during the night, the data were omitted from analysis.

Calculation of the mean absolute relative difference (MARD) and percent absolute relative difference PARD:

The mean absolute relative difference (MARD) for the microneedle CGM sensors was defined as the average percent difference between the microneedle sensor's estimation of blood glucose and reference (YSI) venous blood glucose. The sensors were calibrated using a single point method whereby the current at a time point after stabilisation was calibrated to the venous blood glucose measured at that time point. It is important to note that there was no recalibration over the following 20 hours. This methodology of assessing against a parallel reference glucose measurement (in this case YSI from venous blood) is both well established and routinely reported, in clinical studies in clinical practice, and in regulatory submission.

It was calculated as follows:

$$MARD = \Sigma (Y_{CGMi}-Y_{RBGi}) / (Y_{RBGi}). 100 / n \quad \text{.....eq. (1)}$$

where $Y_{RBG}i$ is the ith reference blood plasma glucose value, $Y_{CGM}i$ is the corresponding sensor measured value at identical time and n is the total number of reference measurements.

The precision of the CGM devices comprising of two sensors on the same devices was assessed using percent absolute relative difference (PARD). The PARD was calculated as described before. [30, 31] Percent absolute relative difference (PARD) for the two CGM sensors in our study was the difference between sensor readings divided by the average of the sensor readings. It was calculated as follows:

$$PARD = \frac{| Y_{CGM_1} - Y_{CGM_2} |}{\text{mean} (Y_{CGM_1}, Y_{CGM_2})} \quad \textit{eq.(2)}$$

where Y_{CGM1} is the sensor derived glucose value for sensor 1, Y_{CGM2} is the sensor derived glucose value for sensor 2 measured at identical time. Both of these values (Y_{CGM1} & Y_{CGM2}) are obtained after single point calibration of the current against the blood glucose value.

Results and Discussion

The studies described here were carried out in accordance with good clinical practice provisions and approved by the Research ethics committee. The study protocol was registered at ClinicalTrials.gov with the number NCT01908530.

Tolerability:

For phase 1, 8 healthy participants were enrolled and their tolerability to the microneedle array structures assessed. The skin response at the microneedles' insertion site, assessed immediately following sensor's removal, was graded as either barely noticeable (7 subjects) or mild erythema (in 1 subject). In all participants, visible skin reaction had completely disappeared within 1 hour of device removal. The median score (interquartile range) on the 100 mm VAS for the microneedle arrays was 10 (1.25-17.5) compared to 30 (20-37.5), for that of the IV cannula, p=0.02.

In Phase 2, the microneedle was inserted into healthy volunteers (8) in the forearm for 24 hours. As seen in figure 4, the pain score obtained for microneedle insertion versus cannula insertion was: Median (SD) Pain Score = 10 (4) vs. 39 (24), p=0.02. The marks due to insertion of the microneedle array as seen in figure 4b disappeared within 3-6 hours of removal. No inflammation or skin irritation due to insertion of devices was reported in any of the 8 volunteers.

Insert Figure 4 here

Studies were also undertaken in participants with T1D, involving comparison of pain scores of microneedles inserted over 24 hours against a commercially available Dexcom CGM and an IV cannula. As seen in figure 4, the median pain score for microneedle CGM was also found to be comparable to the Dexcom CGM but lower than that of the IV cannula.

Optical coherence tomography studies:

OCT images were acquired each to assess the penetration of the microneedles and any axial displacement during use. This revealed no variation in the penetration depths of the microneedles when measured over 24 hours. A summary of results from the OCT images, involving the measurement of the air gap between the base plate and skin, is summarised in Figure 5. As shown in the figure, the median penetration depth is represented by the boxes, the values are shown beneath the box. Also shown are the lower (yellow) and upper (purple) quartile ranges. The whiskers show the largest and smallest values. The Kruskal-Wallis analysis reveals no significant difference in the median penetration depths over the 24hrs of insertion.

Insert Figure 5 here

Performance accuracy

Phase3 participants with T1D showed a wide variation in venous blood glucose concentrations ranging from 2.6 to 20.0 mMol/L (47 to 360 mg/dL). The microneedle devices were tested on 10 participants and the values of the current obtained from 2 independent sensors on the same device were compared against YSI venous blood glucose. 2 of the 10 devices, showed no functionality post *in vivo* studies. One plausible reason for this could be a

strong dose of gamma ray irradiation causing damage to the sensors during the sterilisation process, all 2 failed sensors were from the same sterilisation batch.

Figure 6 is a representative of a chronoamperometric measurement obtained from a microneedle array CGM device where two of the sensors have been biased. In a double axis plot, the currents generated by the microneedle array CGM sensors and the glucose concentrations from venous blood have been plotted over a period of 21hr. The variations in the current values of the two sensors on the same device is due to the difference in area of the microneedle electrodes introduced during the masking step.[19]

In this study, the currents were converted to glucose values retrospectively by single point calibration of the maximum current and corresponding YSI glucose value. As seen with most the CGM electrochemical sensing devices, there is a time[32] interval during which the sensor stabilises, in this instance, most of the sensors stabilised in two hours. Only data points after the sensor stabilisation time were used for the CEG plot. The MARD value in this participant study was 4%, while the PARD value between two sensors on this device was 1%.

Insert Figure 6 here

A summary of all 205 data points obtained from the Phase 3 study are shown in the CEG plot in Figure 7. From the CEG plot, it appears that the microneedle CGM performance is clinically acceptable (Zone A and B). The percent values in the different zones of the CEG plot are given in the figures. The analysis shows that 96.4% points fall within clinically acceptable zones A and B and 3.6% fall in zone C. None of the points fell in zones D and E. The MARD values calculated for the Phase 3 studies in subjects with T1D was 9%.

Insert Figure 7 here

Discussion

Microneedle based continuous glucose monitoring systems are gaining interest because of the potential advantages they offer. The preliminary results shown here demonstrates how solid microneedle arrays functionalised to glucose sensing devices can provide clinically acceptable results over durations of up to 24 hours without inflammation and with minimal discomfort. The data presented are first time in man and, where technical problems were encountered, such as disconnection, data were excluded so further technical development is

required to produce a robust ambulatory device. However, accuracy and performance are comparable to commercially available devices in studies in the clinical research facility. Further clinical studies in the home over longer duration are planned.

The chronoamperometric data indicated lag times of up to 15 minutes in some cases and in some cases negligible lag times. Basic filtering algorithms involving removal of the two extreme values, was used for processing the data on the PCB potentiostat. The calibration algorithms will be further improved to track the sensor behaviour and offset the lag time and sensor drift.[33]

The functionalization of the microneedle arrays involves use of electropolymerisation to form a thin film of polyphenols with the glucose oxidase enzyme entrapped in it. Adoption of technologies such as automated dispensing of hydrogels will offer a scalable technology and better tissue adhesion to minimise movement artefacts caused by lateral displacement. We are also exploring means that do not affect the performance of the microneedle CGM sensors on sterilisation the microneedle CGM devices. The ultimate aim of this project is to provide microneedle CGM sensors at daily costs comparable to the use of glucose finger stick strips whilst offering the value of continuous glucose measurements.

Conclusions

In conclusion, the devices were well tolerated and the current output measured showed good correlation with venous blood glucose concentrations. Compared to commercially available subcutaneous CGMs that require an applicator device to implant the sensors, the intradermal CGM devices reported here could be easily inserted on the forearm under moderate thumb pressure, or could be incorporated into the back of a watch. The OCT measurements of the microneedle penetration depths at regular intervals have indicated no axial displacement.

These pilot studies on the prototype device show highly acceptable clinical performance of the sensor proving the feasibility of the approach of using solid microneedles seated in the dermal ISF, a feature that is novel to the microneedle design. This sets up the sensors for further clinical evaluation in a larger number of participants with T1D.

References:

1. T. J. D. R. F. C. G. M. S. Group, *New England Journal of Medicine*, 2008, **359**, 1464-1476.
2. K. M. Miller, D. Xing, W. V. Tamborlane, R. M. Bergenstal and R. W. Beck, *J Diabetes Sci Technol*, 2013, **7**, 963-969.
3. G. Diabetes Research in Children Network Study, *Pediatric Diabetes*, 2009, **10**, 91-96.
4. A. Jina, M. J. Tierney, J. A. Tamada, S. McGill, S. Desai, B. Chua, A. Chang and M. Christiansen, *Journal of Diabetes Science and Technology*, 2014, **8**, 483-487.
5. R. Donnelly and D. Douroumis, *Drug Deliv Transl Re*, 2015, **5**, 311-312.
6. Y. C. Kim, J. H. Park and M. R. Prausnitz, *Adv Drug Deliver Rev*, 2012, **64**, 1547-1568.
7. H. L. Quinn, M. C. Kearney, A. J. Courtenay, M. T. C. McCrudden and R. F. Donnelly, *Expert Opin Drug Del*, 2014, **11**, 1769-1780.
8. C. Meyerhoff, F. J. Mennel, F. Bischof, F. Sternberg and E. F. Pfeiffer, *Horm Metab Res*, 1994, **26**, 538-543.
9. M. L. Rogers, D. Feuerstein, C. L. Leong, M. Takagaki, X. Z. Niu, R. Graf and M. G. Boutelle, *Acs Chem Neurosci*, 2013, **4**, 799-807.
10. M. J. Tierney, J. A. Tamada, R. O. Potts, R. C. Eastman, K. Pitzer, N. R. Ackerman and S. J. Fermi, *Annals of Medicine*, 2000, **32**, 632-641.
11. H. Chuang, E. Taylor and T. W. Davison, *Diabetes Technology & Therapeutics*, 2004, **6**, 21-30.
12. E. Eltayib, A. J. Brady, E. Caffarel-Salvador, P. Gonzalez-Vazquez, A. Z. Alkilani, H. O. McCarthy, J. C. McElnay and R. F. Donnelly, *Eur J Pharm Biopharm*, 2016, **102**, 123-131.
13. A. El-Laboudi, N. S. Oliver, A. Cass and D. Johnston, *Diabetes Technology & Therapeutics*, 2013, **15**, 101-115.
14. N. S. Oliver, C. Toumazou, A. E. G. Cass and D. G. Johnston, *Diabetic Med*, 2009, **26**, 197-210.
15. P. R. Miller, R. J. Narayan and R. Polsky, *J Mater Chem B*, 2016, **4**, 1379-1383.
16. T. M. Rawson, S. Sharma, P. Georgiou, A. Holmes, A. Cass and D. O'Hare, *Electrochem Commun*, 2017, **82**, 1-5.
17. A. E. Cass and S. Sharma, *Methods Enzymol*, 2017, **589**, 413-427.
18. A. R. Moniz, K. Michelakis, J. Trzebinski, S. Sharma, D. G. Johnston, N. Oliver and A. Cass, *J Diabetes Sci Technol*, 2012, **6**, 479-480.
19. S. Sharma, Z. Y. Huang, M. Rogers, M. Boutelle and A. E. G. Cass, *Anal Bioanal Chem*, 2016, **408**, 8427-8435.
20. S. Sharma, A. Saeed, C. Johnson, N. Gadegaard and A. E. Cass, *Sens Biosensing Res*, 2017, **13**, 104-108.
21. J. Trzebinski, S. Sharma, A. R. B. Moniz, K. Michelakis, Y. Y. Zhang and A. E. G. Cass, *Lab Chip*, 2012, **12**, 348-352.
22. J. R. Castle, A. Pitts, K. Hanavan, R. Muhly, J. El Youssef, C. Hughes-Karvetski, B. Kovatchev and W. K. Ward, *Diabetes Care*, 2012, **35**, 706-710.
23. M. Boschmann, F. P. Murphy and J. G. Krueger, *Dermatology*, 2001, **202**, 207-210.
24. R. F. Donnelly, T. R. R. Singh and A. D. Woolfson, *Drug Delivery*, 2010, **17**, 187-207.
25. M. Reddy, P. Herrero, M. El Sharkawy, P. Pesl, N. Jugnee, H. Thomson, D. Pavitt, C. Toumazou, D. Johnston, P. Georgiou and N. Oliver, *Diabetes Technol Ther*, 2014, **16**, 550-557.
26. P. Herrero, M. El Sharkawy, P. Pesl, M. Reddy, N. Oliver, D. Johnston, C. Toumazou and P. Georgiou, *Biomed Circ Syst C*, 2014, 172-172.
27. W. L. Clarke, D. Cox, L. A. Gonder-Frederick, W. Carter and S. L. Pohl, *Diabetes Care*, 1987, **10**, 622-628.
28. D. Stockl, K. Dewitte, C. Fierens and L. M. Thienpont, *Diabetes Care*, 2000, **23**, 1711-1712.
29. J. Bondia, C. Tarin, W. Garcia-Gabin, E. Esteve, J. M. Fernandez-Real, W. Ricart and J. Vehi, *J Diabetes Sci Technol*, 2008, **2**, 622-629.
30. T. Bailey, H. Zisser and A. Chang, *Diabetes Technology & Therapeutics*, 2009, **11**, 749-755.

31. H. C. Zisser, T. S. Bailey, S. Schwartz, R. E. Ratner and J. Wise, *Journal of diabetes science and technology (Online)*, 2009, **3**, 1146-1154.
32. D. C. Klonoff, *Diabetes Care*, 2005, **28**, 1231-1239.
33. A. Facchinetti, *Sensors-Basel*, 2016, **16**.

Acknowledgements

This is a summary of independent research partly funded by the National Institute for Health Research (NIHR)'s Invention for Innovation (i4i) Programme (Grant Reference Number II-LA-0313-20004). The views expressed are those of the author(s) and not necessarily those of the NHS, the NIHR or the Department of Health.

We would like to acknowledge the support from clinical staff at the NIHR Imperial Clinical Research Facility. Contributions by Professor Nikolaaj Gadegaard, Glasgow University, Professor Owen Guy & Dr Gareth Blaney, Swansea University and Dr Kostis Michelakis, Surrey University towards device fabrication and metallisation are greatly appreciated. We also acknowledge Dr Jon Holmes, Michelson Diagnostics for his help with optical coherence tomography measurements.

Conflict of Interest Disclosure: The authors declare no competing financial interest.

Captions:

Figure 1: Showing: (1a) Clinical study plan showing the three different phases (1b) schematic of the microneedle sensor (1c) an image of the microneedle arrays showing the four arrays representing two working electrodes, one reference and one counter electrode.

Figure 2: Showing (2a) metallised and (2b) specially designed microneedle arrays to obtain OCT images and (2c) an OCT image used to look at the axial displacement of the microneedles.

Figure 3: Showing the instrumentation used in different phases of the clinical study.3(a) CHI potentiostat on a trolley; 3(b) Emstat potentiostat; 3(c) potentiostat on a printed circuit board.

Figure 4: Showing the pain scores for microneedles during Phases 1,2 and 3. (Inset) Showing the marks seen after the microneedle array device is removed.

Figure 5: The box shows the median penetration depth (also as a value beneath the box), the lower (yellow) and upper (purple) quartile ranges. The whiskers show the largest and smallest values. At the bottom is the scale of the values in **mm**.

Figure 6: Showing a double axis plot representing chronoamperometric measurements from two sensors (black: working electrode 1; red working electrode 2) on the same device versus YSI venous blood (represented as blue stars).

Figure 7: Clarke error grid analysis comparing clinical performance of the IC CGM sensors in T1D subjects.96.6% values fall in zones A and B whilst the remaining 3.4% fall in zone C.

Figure 1.

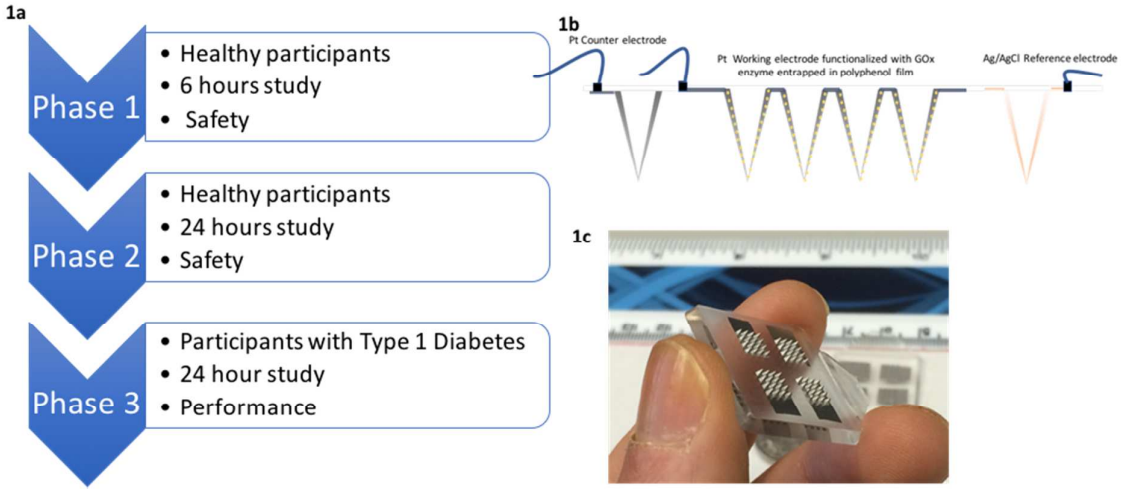

Figure 2

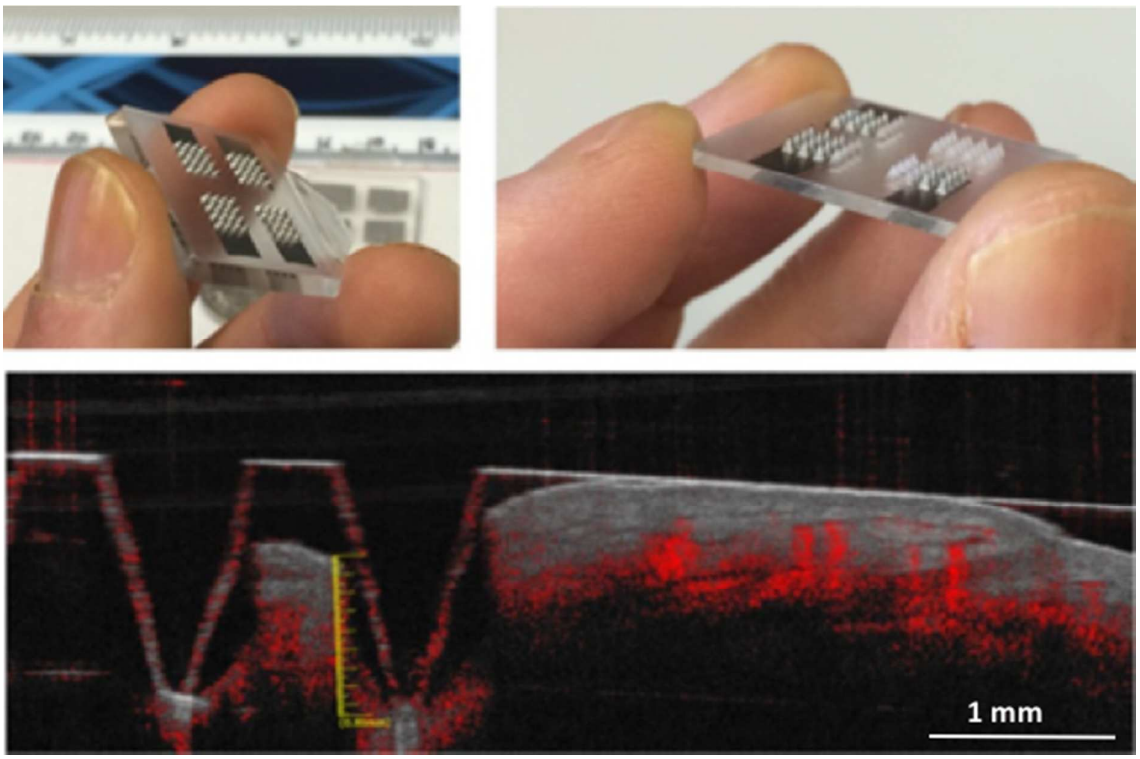

Figure 3

Figure 4:

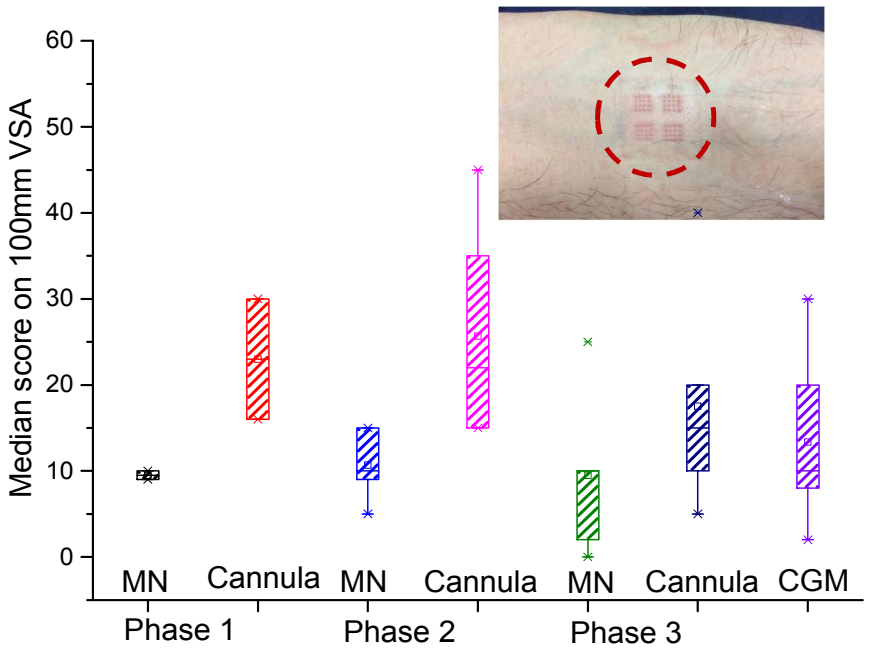
Median score on 100mm VSA
60
50
40
30
20
10
0
MN
Cannula
MN
Cannula
MN
Cannula
CGM
Phase 1
Phase 2
Phase 3

Figure 5:

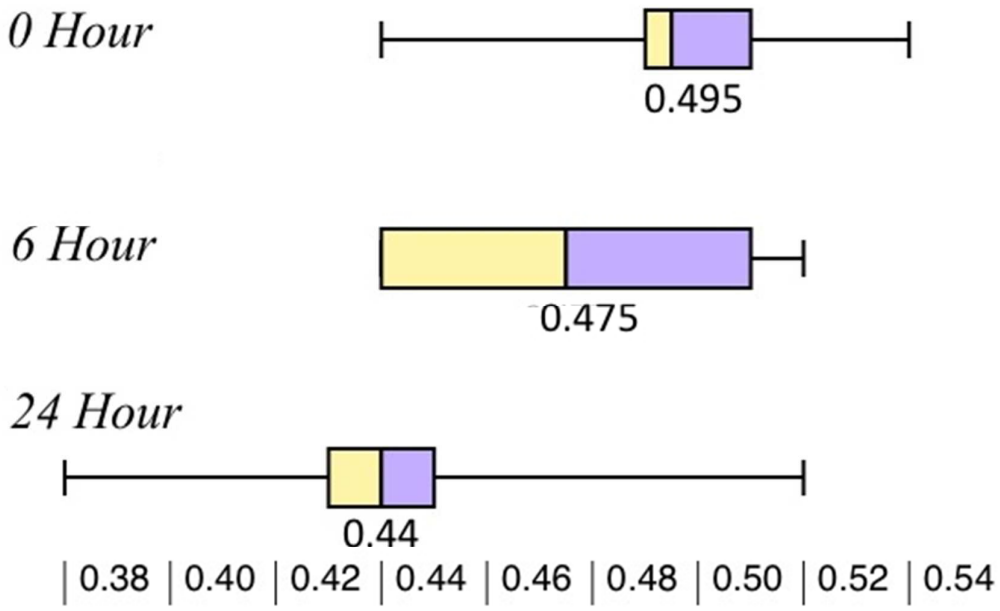
0 Hour
0.495
6 Hour
0.475
24 Hour
0.44
0.38
0.40
0.42
0.44
0.46
0.48
0.50
0.52
0.54

Figure 6:

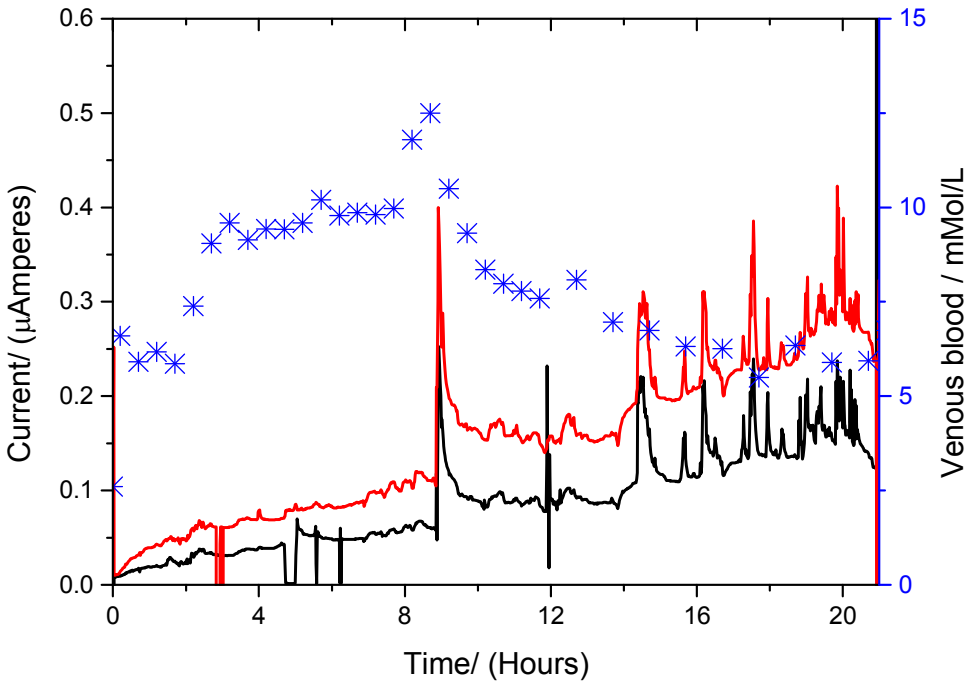
Current/ (μAmperes)
Venous blood / mMol/L
Time/ (Hours)
0.0
0.1
0.2
0.3
0.4
0.5
0.6
0
5
10
15
0
4
8
12
16
20

Figure 7:

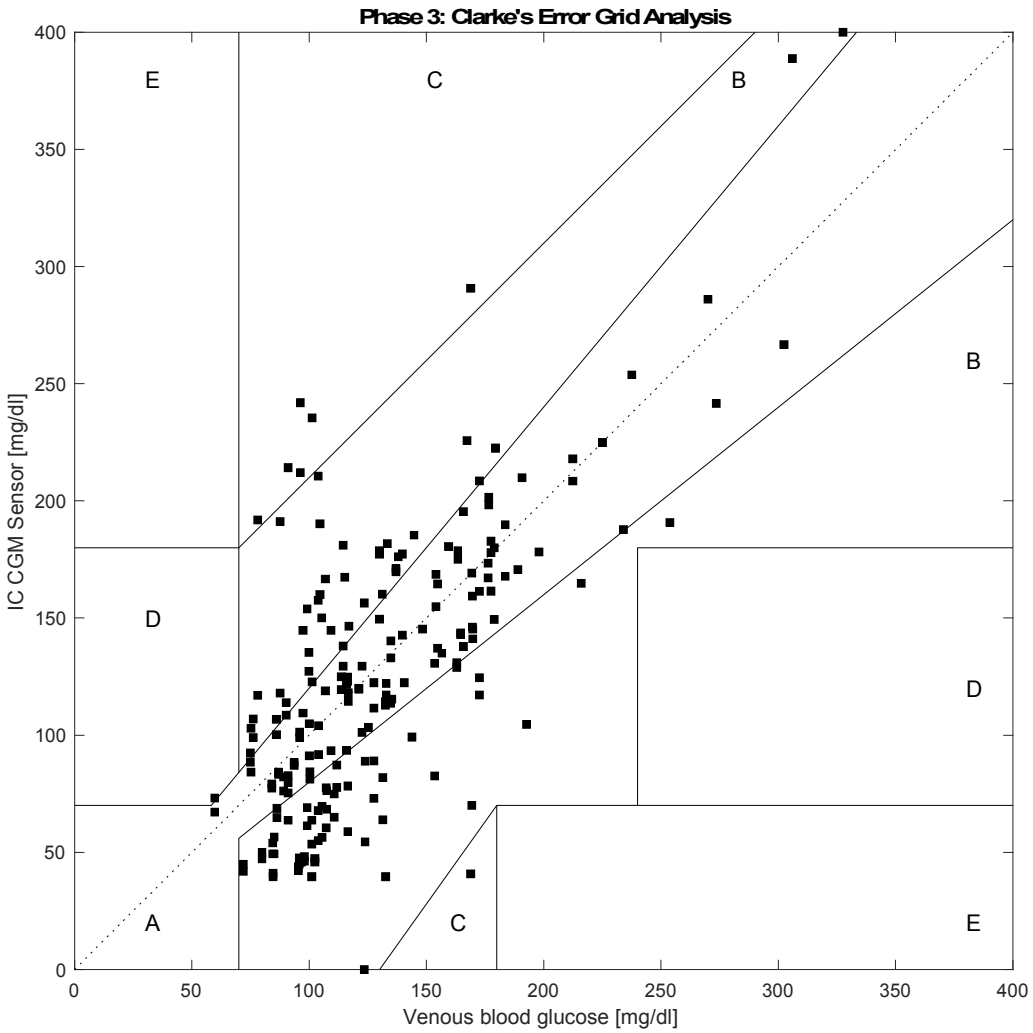
Phase 3: Clarke's Error Grid Analysis
E
C
B
B
D
D
A
C
E
IC CGM Sensor [mg/dl]
Venous blood glucose [mg/dl]
0
50
100
150
200
250
300
350
400

Graphic entry for the Table of Contents (TOC)